Phase Unwrapping Techniques for SAR Interferometry: A Comprehensive Review

Alka Saini[1]*, Deepak Mishra[2]and V Manavala Ramanujam[1]

[1]Space Application Centre, ISRO, Ahmedabad, India
[2]Department of Avionics, Indian Institute of Space Science and Technology, India
*Corresponding Author's email: alkasaini@sac.isro.gov.in

Abstract

Synthetic Aperture Radar (SAR) Interferometry (InSAR) represents one of the most widely employed remote sensing methodologies for precise topographical mapping and ground deformation monitoring. InSAR harnesses the phase disparity between a pair of co-registered SAR images, termed the interferometric phase (ψ). The two-dimensional depiction of ψ is referred to as the interferogram, conventionally measured modulo 2π. To derive topographic elevations and ground deformations from the interferogram, it is imperative to transform the wrapped interferometric phase into an absolute phase field (φ) by appending the correct multiple of 2π to each fringe (2πk, where k denotes the wrap count, such that $\phi(x,y) = \psi(x,y) + 2\pi k(x,y)$). However, this undertaking is inherently ill posed, necessitating the incorporation of additional constraints for robust solutions. Conventionally, the Itoh's condition is applied, limiting the phase discrepancy between neighboring pixels to the range of [-π, π]. The phase unwrapping (PU) process aims to extract the continuous phase (ϕ) from its wrapped counterpart(ψ), which lies within the interval (-π, π]. Traditional Spatial Phase Unwrapping Methods encompass path-following, Minimum Norm-based, and network-based strategies. Recent strides made in advanced unwrapping methodologies, including Deep Learning-driven Regression, Deep Learning-driven Wrap Count determination, and Deep Learning-facilitated De noising techniques. This paper provides an overview of various phase unwrapping algorithms. It identifies key research areas and emphasizes the need for robust phase unwrapping techniques to enhance the accuracy and reliability of SAR Interferometry for Earth observation and geospatial analysis.

Keywords InSAR, Phase Unwrapping (PU), Interferogram (IFG), Residue, Digital Elevation Model (DEM), Single Look complex (SLC)

Introduction

Interferometric Synthetic Aperture Radar (InSAR) is a radar technique used in geodesy and remote sensing to create digital elevation maps and detect surface deformations. It can detect millimeter-scale changes in deformation over various time frames, making it valuable for monitoring natural hazards like earthquakes, volcanoes, and landslides. To generate a DEM from Single look complex (SLC) images in InSAR, several steps are involved, including co-registration, resampling, filtering, interferogram (IFG) generation, coherence calculation, Phase Unwrapping (PU), slant-to-height conversion, and geo-coding. The accuracy and reliability of the results are directly impacted by PU [Chen & Zebker, 2001, 2002]. InSAR creates an IFG by multiplying two SAR images S1 & S2 shown in Eq (1) & (2) at different

times, representing the phase difference between corresponding pixels in co-registered SLC images.

$$S_1 = a_1 exp^{(i4\pi R_1/\lambda)}, S_2 = a_2 exp^{(i4\pi R_2/\lambda)} \quad (1.1)$$

Where a1, a2 = complex reflectivity, R1, R2 is range from antenna to surface, $\lambda =$ wavelength,

$$(s_1)(s_2^*) = a_1 a_2 exp^{(i4\pi(R_1 - R_2)/\lambda)} = s(t) \quad (1.2)$$

Phase Difference is proportional to the effective difference in range, which in turn depends on satellite geometry, topography [Bamler & Hartl, 1998] and provides crucial information about surface deformation and elevation changes, this. The relationship between topographical height and absolute phase is as follows:

$$h(p) = \frac{\lambda \, \mathrm{R} \sin\theta \phi(p)}{4\pi B_{per}} \quad (1.3)$$

Where $h(p)$ the topographical height of the pixel, *R* is the slant range of the pixel, θ is the incidence angle and B_{per} is the perpendicular baseline. Wrapped phase is obtained from IFG that varies from $-\pi \leq \psi(p) - \psi(p-1) < \pi$, and unambiguous absolute phase can be obtained by Eq. (2):

$$\phi(p) = \psi(p) + 2\pi k(p) \quad (1.4)$$

The biggest difficulty of 2-D PU is that there are two unknown variables $\psi(p)$ and $k(p)$ in Eq. (1.4). Therefore, we cannot obtain the absolute phase $\psi(p)$ to recover the topographical height $h(p)$ only through Eq. (1.3). To obtain the unique solution of (1.3), the phase continuity assumption (or Itoh condition) [K. Itoh., 1982] was proposed and applied to almost all 2-D PU methods. The phase continuity assumption assumes that the phase differences between adjacent pixels do not exceed π. Under this assumption, we can correctly estimate the absolute phase gradient information, which is obtained by the following formula:

$$\nabla\phi(p-1) = \begin{cases} \psi(p) - \psi(p-1), & \text{if } |\psi(p) - \psi(p-1)| \leq \pi \\ \psi(p) - \psi(p-1) - 2\pi, & \text{if } \psi(p) - \psi(p-1) > \pi \\ \psi(p) - \psi(p-1) + 2\pi, & \text{if } \psi(p) - \psi(p-1) < -\pi \end{cases}$$

Where, $\nabla\phi$(p-1) is the estimated absolute phase gradient between adjacent pixels, p and p-1.

The interferometric phase (IFG) in real applications often contains noise and large deformation gradients, resulting in phase discontinuities. These discontinuities challenge PU methods as they violate the assumption of phase continuity. To estimate local topography, an unwrapping procedure is necessary. The goal of PU is to recover the integer number of cycles k $\in\mathbb{Z}$ to add to the wrapped phase Ψ(p) to obtain an unambiguous phase value Φ(p) for each image pixel. This problem is more difficult and numerous solving techniques have been proposed in the literature.

Materials and Methods

This section of the article offers a comprehensive assessment of phase unwrapping algorithms, which can be categorized into three main types: Path-following methods, Optimization based methods and Deep learning-based methods. Here, we will provide concise descriptions of each method being examined, emphasizing their core principles.

Path-Following Methods: Path-following methods aim to integrate estimated phase gradients to enhance accuracy while traversing a grid path and making incremental phase value adjustments. However, they do not directly address residue issues but incorporate them during unwrapping. To handle residues and prevent path-dependent results, cut lines and branch cuts (Goldstein et al., 1988) are introduced. Table-1 provides an overview of the Path-Following Phase Unwrapping (PU) techniques.

Table 1 Overview of Various Path-Following Phase Unwrapping (PU) Techniques.

Path following Algorithm	Description
Branch-Cut Algorithm	Detects discontinuities in the wrapped phase field. Identifies residues as +1 or -1 charges based on phase differences along closed paths. Utilizes branch cuts as impassable barriers during path integration. Requires careful placement of branch cuts.
Quality Guided Methods	Leverages quality maps to guide integration paths. Addresses residues in low-quality regions, prioritizing higher-quality pixels for phase unwrapping. Aims to mitigate the potential misplacement of branch cuts, which is a challenging problem in branch cut. When a high-quality map is not available, Goldstein's algorithm demonstrates superior performance
Mask Cut	Combines quality maps with branch cuts (Goldstein's algorithm) to form a hybrid approach. Quality maps guide the placement of branch cuts, enhancing the accuracy of the unwrapping process.

Residue is the discontinuity in IFGs and defined by Eq. (1.5)

$$R_{mn} = \nabla^x \psi_{mn} - \nabla^x \psi_{m,n+1} + \nabla^y \psi_{m+1,n} - \nabla^y \psi_{mn} \tag{1.5}$$

Where $\nabla^x\psi$ and $\nabla^y\psi$ are the derivatives of the M×N wrapped phase in the vertical and the horizontal direction.

Quality Guided Algorithms prioritize pixels with higher quality values during phase unwrapping order [M. Roth, 1995], utilizing metrics like Correlation coefficient, Pseudocorrelation, Maximum gradient, and Phase derivative variance (Eq. 1.6) [Ghiglia & Pritt. (Chap.4), 1998].

$$v(m,n) = \frac{\sqrt{\left(\sum(\nabla^x\psi_{ij} - \overline{\nabla^x\psi_{mn}}\right)^2} + \sqrt{\left(\sum\left(\nabla^y\psi_{ij} - \overline{\nabla^y\psi_{mn}}\right)^2\right.}}{N^2} \quad (1.6)$$

Where each sum of index (i, j) ranges over the N ×N window centered at the pixel (m, n).$\nabla^x\psi_{ij}$ and $\nabla^y\psi_{ij}$ are derivatives of wrapped phase. Terms $\overline{\nabla^x\psi_{mn}}$ and $\overline{\nabla^y\psi_{mn}}$ are averages of these partial derivatives in the N ×N window.

The Mask Cut [Ghiglia & Pritt, 1998] algorithm distinguishes itself from quality-guided methods by following lower quality pixels from one residue to another until a balance is achieved via regions of low-quality pixels known as mask cuts. Mask Cut does not minimize the length of mask cuts but incorporates a thinning operation for optimization.

Optimization Based Methods: Optimization-based methods in phase unwrapping utilize mathematical functions and algorithms to minimize phase discontinuities and obtain a more accurate unwrapped phase map.

Minimum Norm Methods: Minimum norm methods employ a global approach, optimizing the entire interferogram image, unlike path following techniques, which operate, on a local scale. The Minimum L^p Norm approach in minimum norm methods aims to minimize the difference between absolute phase derivatives and wrapped phase derivatives, resulting in an absolute phase solution as Eq (1.7). The objective is to obtain an unwrapped image solution of cost function J_{ij}, shown in Eq (1.8)

$$\hat{\phi} = \underset{\phi}{argmin}\, J_{ij} \quad (1.7)$$

$$J_{ij} = \sum_{i=1}^{M}\sum_{j=1}^{N-1} q_{ij}^{h}|\,\nabla^h\phi_{ij} - \nabla^h\psi_{ij}|^p + \sum_{i=1}^{M-1}\sum_{j=1}^{N} q_{ij}^{v}|\,\nabla^v\phi_{ij} - \nabla^h\psi_{ij}\,|^p \quad (1.8)$$

$$\nabla^h\psi_{ij} = W\left(\psi_{i,j+1} - \psi_{ij}\right), \nabla^v\psi_{ij} = W\left(\psi_{i+1,j} - \psi_{ij}\right), \nabla^h\phi_{ij} = \phi_{i,j+1} - \phi_{ij}, \nabla^v\phi_{ij} = \phi_{i+1,j} - \phi_{ij} \quad (1.9)$$

Eq. (1.9) indicates discrete differentiation; $q_{ij}^{h/v}$ are horizontal and vertical quality measures [H. Lim, W. Xu, & X. Huang, 1995] known as user-defined weights; and the summations include all appropriate rows i and column j. In regions where it is known to exist absolute phase discontinuities, or noise corruption, we can set $q_{ij}^{h/v}$ to lower or zero values and, so, reduce the bad quality phase influence on the unwrapped solution [Ghiglia &. Romero, 1999].

A. L^2 Norm Algorithms/Least squares Methods: The least-squares form (p = 2 in Eq. (1.8)), is a common minimum-norm algorithm, aiming to minimize the square of differences' magnitude. However, it can smooth discontinuities without binary weights. Various algorithms have been developed to approximate the least squares solution by relaxing the discrete domain from $\mathbb{Z}^{mn}\ to\ \mathbb{R}^{mn}$. This relaxation addresses computational challenges and can be done using fast Fourier or cosine transforms or network programming techniques [14, Chap. 5].An exact solution to least squares is developed as a step of the ZπM algorithm in [Jos M. Bioucas-Dias & Gonalo Valadao, 2007], using network programming techniques.LS phase unwrapping can be unweighted or weighted.

Unweighted LS unwrapping: The unweighted least-squares solution to an over-determined set of linear equations is: $G\phi = \rho \quad \Rightarrow \quad G^T G\phi = G^T\rho \;\Rightarrow\; (G^T G)^{-1}G^T G\phi = (G^T G)^{-1}G^T\rho$

Where $\rho_{mn} = (\nabla\psi^x_{mn} - \nabla\psi^x_{m-1,n}) + (\nabla\psi^y_{mn} - \nabla\psi^y_{m,n-1})$ is wrapped phase differences

$$\phi_{ls} = (G^T G)^{-1}G^T\rho \tag{2.1}$$

Where $\boldsymbol{\phi_{ls}}$ is unwrapped phase solution shown in Eq (2.2), and **G** is a geometry matrix which converts phase to wrapped phase differences. The discrete Laplacian operation,$\boldsymbol{G^T G}$, is used to solve partial differential equations in the form of a discrete version of Poisson's equation. Fast Fourier Transform (FFT) algorithms stitch mirror images of the phase to create periodicity, allowing for easy solution using Fourier-transform techniques.

Weighted least-squares algorithms: use quality maps to avoid branch points, providing a more robust. They solve overdetermined linear equations: $WG\phi = W\rho \quad \Rightarrow \quad G^T W^T WG\phi = G^T W^T W\rho$

$$Q\phi = s \tag{2.2}$$

Where $Q = G^T W^T WG$ & $s = G^T W^T W\rho$ and W is a matrix of weights, the vector s contains weighted phase differences with discrete Laplacian operation thus Eq. (2.2) cannot be solved using unweighted LS techniques like FFT-based algorithms due to its computationally intensive and time-consuming nature [Pritt, M.D., 1994]. The Picard method and Preconditioned Conjugate Gradient (PCG) are two methods for solving weighted LS problems, but the Picard method is impractical due to its many iterations, while PCG is faster.

B. L^1 Norm Algorithms: In cases when there are many outliers (unwrap errors), the L^1-norm is more resilient than the L^2-norm. The algorithms with the minimal L^1-norm retain discontinuities better than those with the L^2-norm.

Flynn's Minimum Weighted Discontinuity Method: The core concept of Flynn's approach [Flynn, T, 1997] is to select between the possible unwrapped images, the one that minimizes discontinuities. This method operates by applying iteratively an elementary step of partitioning the image in two connected regions and then, adding a 2π phase to one of them, such that the weighted sum of

discontinuities decrease. Flynn method calculates the weighted sum of the magnitudes of the phase discontinuities (horizontal (h_{ij}) and vertical jumps (v_{ij}) in Phase) and aims to place these discontinuities in appropriate locations.

The goal of Flynn's algorithm is to minimize following Cost function Z_{mn} mentioned in Eq (2.3), which helps in obtaining a more accurate unwrapped phase map.

$$Z_{mn} = \sum q^v_{i,j}\left|v_{i,j}\right| + q^h_{ij}\ \left|h_{i,j}\right| \tag{2.3}$$

Where $v_{ij} = \left\lfloor \frac{\phi_{ij} - \phi_{i-1,j} + \pi}{2\pi} \right\rfloor$ $h_{ij} = \left\lfloor \frac{\phi_{ij} - \phi_{i,j-1} + \pi}{2\pi} \right\rfloor$

The phase unwrapping max-flow algorithm (PUMA) PUMF Approach: Bioucas-Dias and Gonçalo Valadão introduced an energy-minimization framework for PU, in order to overcome drawback associated to minimum L^2-Norm by setting 0 ≤ p ≤ 1. They used graph-cut optimization and max-flow/min-cut calculations to tackle binary optimization tasks. The primary objective is to identify the integer image k that minimizes the energy function $E(K|\psi)$[J.M B. Dias & J.M.N. Leitao, (2002)]. PU-max-flow is well suited for the minimum norm category of phase unwrapping algorithms, addressing phase discontinuities and incorporating nonconvex discontinuity-preserving potentials. $E(K|\psi)$ is given as in Eq (2.4):

$$E(K|\psi) = \sum_{i,j\in\mathbb{Z}_1} V\left(\nabla^h \phi_{ij}\right) v_{ij} + V\left(\nabla^v \phi_{ij}\right) h_{ij} \tag{2.4}$$

Where $\mathbf{k} \equiv \{k_{ij} : (i,j) \in \mathbb{Z}_0\}$ wrap-count image,$(i,j) \in \mathbb{Z}_1 \equiv \{i = 0,1,\cdots,M, j = 0,1,\cdots,N,$ and $hij, vij \in \{0,1\}$ are horizontal and vertical discontinuities, respectively; wheras $hij, vij = 0$ is a a discontinuity, V (·) is the clique potential.

Network programming-based Methods: The reformulation of the PU problem enables network optimization techniques [Ahuja93], particularly in small, disconnected urban areas. This has led to a growing demand for global optimization and automated unwrapping approaches, prompting InSAR network programming concepts [M. Costantini (http://www.geo.unizh.ch/ rsl/fringe96/papers/costantini].

The Minimum Cost Flow (MCF) and Triangulation Network: MCF algorithm introduced by Costantini [Costantini, 1998] aims to minimize total cost by maximizing flow in each arc. The algorithm calculates the smallest error between the wrapped and unwrapped phase gradients, based on phase deviations$(k_1, k_2,)$. The wrapped phase gradient and the unwrapped phase gradient are obtained by the Eq. (1.9) and there is a $2\pi k$ phase difference between them shown in in Eq (2.5), so the unwrapped phase can be obtained by Eq (2.6) & (2.7):

$$\nabla^v \phi_{ij} \ = \nabla^v \psi_{ij} \ + 2\pi k_1(\mathrm{I,j}) \in \mathrm{S}_1 \equiv \{i = 0,1,\cdots,M-2, j = 0,1,\cdots,N-1\},$$

$$\nabla^h \phi_{ij} = \nabla^h \psi_{ij} + 2\pi k_2(\mathrm{i,j}) \in \mathrm{S}_2 \equiv \{i = 0,1,\cdots,M-1, j = 0,1,\cdots,N-2\} \tag{2.5}$$

The MCF algorithm consists of establishing the minimum objective function,

$$min\left\{\sum_{i=0}^{M-2}\sum_{j=0}^{N-1} w_1 |\, k(i,j)\right| + \sum_{i=0}^{M-1}\sum_{j=0}^{N-2} w_2 |\, k_2(i,j)\left|\right\} \tag{2.6}$$

Where w_1 and $w_2$represent the reliability of the pixel, $w_1, w_2 \in [0,1]$, solving the k value by the constraints as follows:

$$k_1(\mathrm{I,j}+1) - k_1(\mathrm{I,j}) + k_2(\mathrm{i}+1,\mathrm{j}) + k_2(\mathrm{I,j}) = \nabla^v \psi_{ij} \ - \nabla^v \psi_{i,j+1} - \nabla^h \psi_{ij} + \nabla^h \psi_{i+1,j} \tag{2.7}$$

Statistical-Cost, Network-Flow Algorithm for Phase Unwrapping (SNAPHU): Chen and Howard A. Zebker presented a PU technique that is based on maximum a posteriori probability (MAP) estimation and nonlinear network flow methods. They defined an objective function as Eq (2.8):

$$min\left\{\sum_k g_k(\nabla\phi_k - \nabla\psi_k)\}\right\} \tag{2.8}$$

Where $\nabla\phi_k$ is unwrapped and $\nabla\psi_k\, is$ wrapped Gradients. Each gradient corresponds to an independent cost function $g(.)$ shown in Eq (2.9) and total cost of the objective function is the sum of all the arc costs. The cost functions are formed from the negative logarithms of the unwrapped-gradient probability density functions (PDFs):

$$g_k(\nabla\phi_k, \nabla\psi_k) = -\log\left(f(\nabla\phi_k|\nabla\psi_k, I, \rho)\right) \quad (2.9)$$

Here, $f(.)$ represents the conditional PDF of a particular unwrapped gradient given the observed wrapped gradient, image intensity (I), and interferometric correlation(ρ). In challenging scenarios like topographic SAR IFGs with layover, rough terrain, and low coherence, SNAPHU algorithm performs exceptionally well, outperforming other algorithms. Even in a differential test, IFG related to an earthquake fault, their method appears to produce a consistent unwrapped solution without apparent errors. The algorithm's accuracy and reasonable efficiency make it a worthwhile choice for specific unwrapping applications till now [Chen & Zebker, H.A., 2000, 2001, 2002].

To verify the effectiveness of our forthcoming Deep learning model, we intend to utilize the unwrapped IFG obtained through the SNAPHU approach.

Deep Learning Based: Incorporating deep learning for PU presents several advantages, even when effective traditional methods exist. Deep learning can handle complex and noisy phase patterns, generalize across diverse datasets, and adapt to specific PU scenarios with ease. It offers automation, speed, and integration possibilities, reducing the need for manual intervention and potentially accelerating the process. Furthermore, deep learning encourages research and development in PU techniques, providing room for innovation and continuous improvement. The widely adopted approach for PU is the deep Learning based Wrap Count method (DLWC). This method treats PU as a classification or segmentation problem, treating each pixel's wrap count as a distinct class label. Another deep regression method (DREG) uses neural networks to learn mapping between wrapped and absolute phases, improving accuracy and anti-noise capability. The research work of some scholars focusing on DLWC and DREG methods is presented in Table 2.

The PU may be affected by the error of the denoising step algorithm if the denoising and unwrapping algorithms are improved separately [Hongxing et al., 2015]. Two solutions have been proposed to solve this issue: adding anti-noise ability and robustness to the PU algorithm or adopting integrated denoising and unwrapping methods [Zhou et al., 2021a; Zhou et al., 2021b]. Zhou, Yu, and Lan in 2020 proposed Pgnet, that was designed to acquire phase gradient characteristics from extensive training images, encompassing varying noise levels and topographic features. Notably, Pgnet exhibited superior performance compared to conventional 2-D phase unwrapping (PU) techniques. Furthermore, a One-step 2-D PU technique using PU-GAN treats 2-D PU as an image-to-image translation challenge and surpasses existing model-based and learning-based 2-D PU methods. It leverages a U-Net architecture for generator generation and Patch-GAN for discriminator learning [Zhou et al., 2022]. PUnet, a robust framework amalgamating U-net, attention mechanism, and positional encoding. PUnet demonstrates remarkable accuracy and robustness in accurately unwrapping phases from wrapped phases, even in the presence of noise [Liu et al. 2023].

While deep learning-based phase unwrapping methods have proven effective in optical imagery, their applicability to InSAR is impeded by intricate wrapped phase characteristics and low coherence coefficients. Nevertheless, the combination of traditional phase unwrapping methods with deep learning represents a promising avenue for further development in this field. We are also in the process of investigating a resilient and efficient deep learning-based method for addressing the PU challenge, with plans to advance DEM development.

Table2 Research Papers on Deep Learning Methods for Phase Unwrapping.

Research Papers	Methodology (Deep Learning Performed Wrap Count method (DLWC).	Research Papers	Methodology Of Deep-Learning-Performed Regression (DREG) Method
Spoorthi et al. 2018	Phase dataset generation method and used the generated dataset to train a SegNet to predict the wrap count, Post processed by clustering-based smoothness to alleviate the classification imbalance.	G. Dardikman-Yoffe et al., 2020	Introduced DREG method using residual-block-based CNN, verified with congruence, compared with wrap count method. Successfully unwrapped samples with steep gradients, utilized a DCNN to predict the unwrapped images with regression network in simulative cell phase maps
T. Zhang et al., 2019	Purposed 3 steps including segmentation to get wrap count, unwrapping, and refinement. Presents a 2D PU method using DeepLabV3+ DCNN, focusing on noise suppression and strong feature representation.	Perera and De Silva, 2021	Testing phase unwrapping with LSTM networks; focus on performance and applicability.
Junchao Zhang et al., 2019	Efficient segmentation network for class identification and phase discontinuity locations; integration of noise-to-noise denoised network for noisy wrapped phase pre-processing; works well with continuous and discontinuous wrapped phases.	Qin et al., 2020	Utilized larger Res-UNet capacity for PU; improved accuracy despite higher computational cost.
Sica et al., 2020	CNN-based unwrapping method using wrapped phase and coherence map; estimation of wrap count gradient; derivation of unwrapped phase field; interferometric coherence's role in noise characterization and management.	Wang et al., 2019,2022	Introduction and demonstration of deep regression methods; superiority in handling noise and aliasing issues.
Spoorthi et al. 2020	Improved wrap count prediction accuracy; introduction of prior knowledge of absolute phase values and gradients into the loss function.	Xu et al. ,2022	Enhanced accuracy and robustness of end-to-end phase unwrapping with composite loss function and additional skip connections in Res-UNet.

Training and testing data sets: In the context of our research, it is imperative to establish robust benchmark datasets for the purpose of training and evaluating deep learning models, focusing on real SAR data from platforms like Tandem SAR-X, Sentinel-1A/B, and SLC datasets. The Copernicus program's Sentinel-1 satellite constellation is used for data acquisition [Copernicus Open Access Hub, ESA], with Interferometric Wide (IW) Swath mode being the preferred choice for interferometric analysis [ESA TM-19] and land subsidence detection. Two primary methods are employed to create benchmark datasets: generating IFGs from SLC image pairs using the SNAP (Sentinel Application form) toolbox [Sentinel-1User Handbook, ESA] and the state-of-the-art SNAPHU method for PU [Chen & Zebker, 2001], and simulating interferometric phase patterns using an edited Shuttle Radar Topography Mission (SRTM) DEM. These datasets will be valuable resources for deep learning experiments and upcoming SAR missions like NISAR and RISAT. The Alaska SAR Facility's website (https://asf.alaska.edu/how-to/data-basics/datasets-available-from-asf-sar-daac/) provides access to wrapped IFGs and SLC pairs for download. Furthermore, our choice of deep learning techniques for this research stems from the need of automatically extracting intricate patterns and features from SAR data, enabling more accurate and efficient analysis and interpretation.

Results

The Least-Squares (LS) approach seeks to reduce the weighted discontinuities in the unwrapped phase, producing a smoother phase map. However, the LS technique could result in a slightly different unwrapped phase after rewrapping compared to the original IFG, necessitating more iterations to get the desired outcome. Figure 3.1 shows the unwrapped phase of a noisy wave signal after weighted and unweighted least square PU, followed by restoration.

Figure 3.2(a) displays the outcomes of Max flow methods applied to simulated Gaussian data. This approach consistently delivers robust unwrapped phase results, particularly in the presence of mild noise. In contrast, Figure 3.2(b) showcases the results achieved by the cutting-edge SNAPHU algorithm when applied to SLC image pair, as mentioned in the STEP forum (https://forum.step.esa.int). In Figure 3.3(a) and Figure 3.3(b), we depict two distinct scenarios involving the unwrapped phase generation from simulated data with varying noise levels, as discussed by Perera & Silva [Perera & Silva, 2021]. In scenario (a), the Root Mean Square Error (RMSE) stands at 0.8352, whereas in scenario (b), the RMSE is 0.0596, highlighting the algorithm's enhanced performance in the latter case. Moving to Figure 3.4, we present the results of a CNN-Based Coherence-Driven Approach applied to the Wrapped Phase. Figures 3.4(b) and 3.4(c) respectively showcase the Unwrapped Phase outcomes as introduced by Sica & Scarpa [Sica et al. ,2022] with Figure 3.4(b) illustrating the input Coherence data for the network. These results underscore the effectiveness of the CNN-Based Coherence-Driven approach in handling the wrapped phase data.

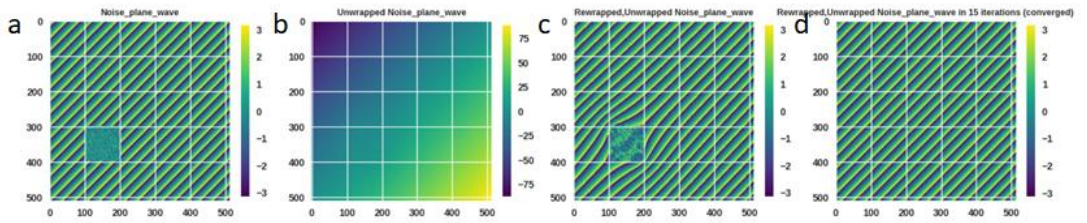

Fig 3.1 (**a**) Original plane wave with uniform noise added. (**b**) Unwrapped Phase of Noisy wave through utilization of Unweighted Least square PU **(c**) Rewrapped phase reconstructed from unwrapped Noisy wave (**b**) Rewrapped Phase from unwrapped Noisy wave in 15th iteration of weighted.

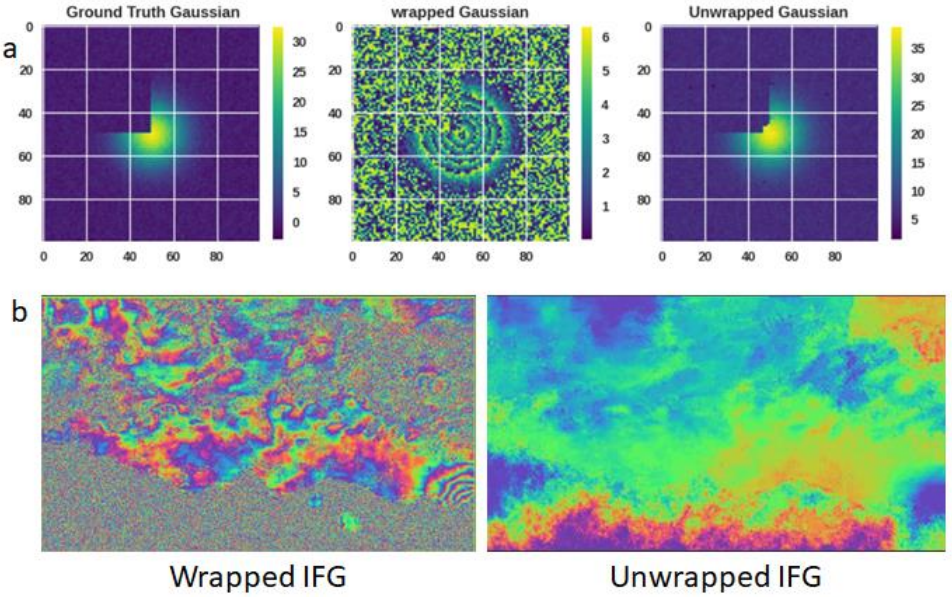

Fig. 3.2 (**a**) (1) Gaussian ground truth data (GT), Wrapped Gaussian and Unwrapped Gaussian(b)Wrapped & Unwrapped IFGs from SNAPHU (Credits: Chen & Zebker, 2000, and TOPS Interferometry Tutorial ,2020 Andreas Braun, Luis Vec).

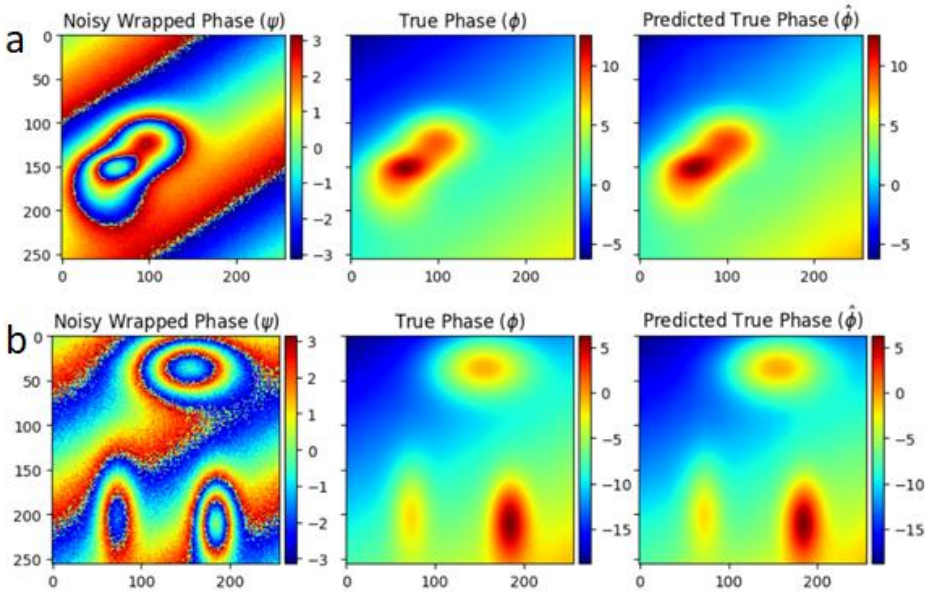

Fig. 3.3 (a) at lesser Noise Level Wrapped Phase, Predicted Unwrapped Phase and GT phase. (b) At more Noise Level Wrapped Phase, Predicted Unwrapped Phase and GT phase.

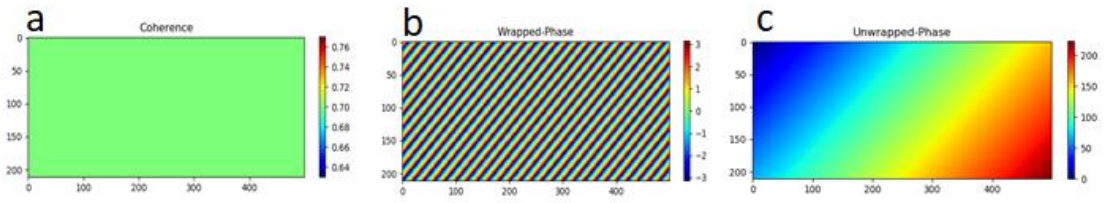

Fig. 3.4 (a) Coherence Input (b) Wrapped Phase (c) Unwrapped Phase from Method of *Sica et.al.,*2022.

Discussion

Although computationally fast, Path following algorithms are not reliable in circumstances of extreme noise. Though the Minimum norm method's performance is noise-resistant, its computations might make them unsuitable for real-time applications While network programming-based techniques yield good outcomes in some situations, most applications employ SNAPHU as a leading. When standard techniques struggle, like in noisy, inconsistent, and aliasing situations, deep learning-based solutions perform well. Deep learning-based Classification, Segmentation and Integrated denoising methods continue to have high precision despite these difficulties. They are producing acceptable results for low noise, and with targeted training, for discontinuous as well. [Wang et al., 2022]. The evaluation of the pluses and minuses of various PU algorithms, as described in Table 3, emphasizes the significance of considering these elements when choosing the best strategy for an InSAR data processing task. When deciding between traditional and deep learning approaches for PU, it is imperative to consider the specific requirements and constraints of the task. Factors such as data availability, computational resources, and desired outcomes should guide this decision. Table 3 provides a detailed summary of the Advantages and Limitations of Phase Unwrapping (PU) Algorithms in the context of InSAR Data Processing.

Conclusions

PU plays a pivotal role in the processing of InSAR data, contributing significantly to various scenarios. Particularly, in scenarios involving longer-time differential IFGs or regions characterized by high coherence and minimal phase noise, the application of multi-looking or filtering techniques can greatly enhance the PU process.

However, as the volume of data continues to grow, the computational efficiency and resilience of the algorithms used become paramount. Identifying potential sources for improving PU methods is a crucial step, yet the optimal combination of these sources remains an ongoing challenge. While it may be uncertain, whether a single PU algorithm can address the majority of PU problems satisfactorily due to their complexity, there should always be an algorithm capable of producing an acceptable result.

Our forthcoming research also aims to Strike the right balance between harnessing the advantages of deep learning and leveraging the proven effectiveness of traditional methods.

Table3 Summary of Advantages and Limitations of PU Algorithms InSAR Data Processing.

Technique	Method	Advantage	Limitation
Path following	Goldstein	simple structure, fast speed, and high accuracy in low-noise regions	Misplacement of branch cut, he unwrapping accuracy is low in high-noise regions
	Quality guided	Best quality maps can be used to reduce effect of discontinuity	Does not identify residues, can encircle unbalanced residues
	Mask cut	Prevents encircling of unbalanced residues	Relies on quality maps to ensure masks are placed and sized properly
Optimization Based	Unweighted (least square/L^2 norm)	Faster execution time	Affected by branch points to a more extent than weighted LS
	Weighted (least square/L^2 norm)	Works best when binary valued weights supplied. Weighted least-squares methods can mitigate residue issues by defining explicit weights to accommodate residues or isolate low signal-to-noise ratio regions.	Many a times Only local minimum solution is obtained
	Flynn (L^1Norm)	Guaranteed to produce a solution minimizing jump counts, obtains global minima	Memory and execution times are higher, if unweighted then it may generate errors
	PUMF (L^1Norm)	PUMA is an exact solver, in particular, of the minimum L^0 norm class of PU algorithms. Even with low-correlation induced discontinuities, PUMA successfully accomplishes a correct PU	PUMA seeks the correct wrap-count image, so it does not intend to get rid of the possible existing noise
	MCF	Allows for robust phase unwrapping in isolated areas of high coherence, particularly in long interval differential IFGs high unwrapping accuracy and strong practicability under low-noise regions	Unwrapping model is usually very complex computationally and requires numerous computational resources. Low unwrapping accuracy and poor robustness in high-noise regions.
	SNAPHU	For particular unwrapping applications, the SNAPHU algorithm is an excellent choice since it performs effectively under challenging conditions and reliably generates unwrapped solutions without errors.	The quality of the unwrapping results are highly dependent on the coherence levels of the IFG., the algorithm running time of SNAPHU is relatively long for bigger tiles of IFG.
Deep Learning based	Deep learning-based Classification Segmentation Methods	The phase value of each pixel in an IFG remains consistent within one fringe period, making PU a classification or segmentation Such a mapping relationship is polarized, i.e., it is either correct or incorrect for each pixel.	Poor noise recognition ability and weak noise resistance
	Deep learning-based regression method	A neural network directly learns the mapping relationship between the wrapped phase and the absolute phase	Inadequate noise reduction and limited feature extraction capacity, the unwrapped phase is incongruent, i.e., each pixel has a small error.
	Integrated Denoising and Unwrapping methods	The neural network can also be used for the invalid pixels filtering	Due to the complex features and high noise level of InSAR images, the computational cost of such methods is generally high

Acknowledgements

We wish to extend my profound gratitude to the Director, SAC at ISRO for their invaluable support of the research endeavours presented in this paper. I am deeply appreciative of the steadfast assistance and guidance provided by Sri. Nikunj Darji and Sri. Bhaskar Dubey throughout the entire process leading to the submission of this work. Furthermore, I would like to convey my heartfelt thankfulness to my family for their unwavering support and encouragement during my academic pursuits.

References

Bamler, R., & Hartl, P. (1998). Synthetic aperture radar interferometry. Inverse Probl. 14(4), R1–R54.

J.M. Bioucas-Dias and G. Valadao, (2007), "Phase unwrapping via graph cuts" in IEEE Trans. Image Process. 16(3).

J.M Bioucas-Dias & J.M.N. Leitao, (2002). The ℤπM algorithm: A method for interferometric image reconstruction in SAR/SAS. IEEE Transactions on Image Processing, 11(4), 408–422.

Chen, C.W., & Zebker, H.A. (2000). Network approaches to two-dimensional phase unwrapping: Intractability and two new algorithms. JOSA A, 17(3), 401–414.

Chen, C.W., & Zebker, H.A. (2001). Two-dimensional phase unwrapping with use of statistical models for cost functions in nonlinear optimization. J. Opt. Soc. Am. A, 18(2), 338–351.

Chen, C.W., & Zebker, H.A. (2002). Phase unwrapping for large SAR interferograms: Statistical segmentation and generalized network models. IEEE Trans. Geosci. Remote Sens. 40.

Costantini, M. (1996). A model-based method for phase unwrapping. IEEE Trans. Med. Imag. 15(6), 893–897.

Costantini, M. (1998). A novel phase unwrapping method based on network programming. IEEE Trans. Geosci. Remote Sens. 36, 813–821.

Dennis C. Ghiglia and Louis A. Romero, "Minimum Lp-norm two-dimensional phase unwrapping," J. Opt. Soc. Am. A **13**, 1999-2013 (1996).

D. Ghiglia and M. Pritt. (1998). Two-Dimensional Phase Unwrapping: Theory, Algorithms, and Software. John Wiley & Sons.

European Space Agency (ESA) Copernicus Scientific Data Hub (http://www.copernicus.eu/.)

European Space Agency (ESA) Sentinel-1 User Handbook (https://sentinels.copernicus.eu/documents/247904/685163/Sentinel-l_User_Handbook).

Ferretti, A., Monti-Guarnieri, A., Prati, C., and Rocca, F. (2007). InSAR principles: Guidelines for SAR interferometry processing and interpretation. Netherlands: ESA: Noordwijk.

Flynn, T. (1997). Two-dimensional phase unwrapping with minimum weighted discontinuity. Journal of the Optical Society of America A, 14(10), 2692–2701.

Francescopaolo Sica, Giuseppe Scarpa, A CNN-Based Coherence-Driven Approach for InSAR Phase Unwrapping", IEEE GEOSCIENCE AND REMOTE SENSING LETTERS, VOL. 19, 2022.

Gili Dardikman-Yoffe, Darina Roitshtain, Simcha K. Mirsky, Nir A. Turko, Mor Habaza, and Natan T. Shaked, "PhUn-Net: ready-to-use neural network for unwrapping quantitative phase images of biological cells," Biomed. Opt. Express 11, 1107-1121 (2020)

G. Valentino, J. A. Briffa, R. Farrugia, A. Fejjari. (2022). Interferometric phase denoising and unwrapping: a literature review. Science Journal of the Malta Chamber of Scientists, 2022.

Ghiglia, D.C., & Romero, L.A. (1994). Robust two-dimensional weighted and unweighted phase unwrapping that uses fast transforms and iterative methods. JOSA A, 11(1), 107–117.

Goldstein, R.M., Zebker, H.A., & Werner, C.L. (1988). Satellite radar interferometry: Two-dimensional phase unwrapping. Radio Sci. 23(4), 713–720.

Guo, Y., Chen, X., & Zhang, T. (2014). Robust phase unwrapping algorithm based on least squares. Opt. Lasers Eng. 63, 25–29.

Herráez, M.A.; Burton, D.R.; Lalor, M.J.; Gdeisat, M.A. (2002). Fast two-dimensional phase-unwrapping algorithm based on sorting by reliability following a noncontinuous path. Appl. Opt. 41, 7437–7444.

H. Lim, W. Xu, & X. Huang. (1995). Two new practical methods for phase unwrapping. In Proceedings of the 1995 International Geoscience and Remote Sensing Symposium-IGARSS'95, pages 196–198, 1995.

H. Yu, Y. Lan, Z. Yuan, J. Xu and H. Lee, "Phase Unwrapping in InSAR : A Review," in *IEEE Geoscience and Remote Sensing Magazine*, vol. 7, no. 1, pp. 40-58, March 2019, doi: 10.1109/MGRS.2018.2873644.

Itoh, K. (1982). Analysis of the phase unwrapping algorithm. Appl. Opt., 21(13), 2470.

Junchao Zhang, Xiaobo Tian, Jianbo Shao, Haibo Luo, and Rongguang Liang, "Phase unwrapping in optical metrology via denoised and convolutional segmentation networks," Opt. Express **27**, 14903-14912 (2019)

Kaiqiang Wang, Ying Li, Qian Kemao, Jianglei Di, and Jianlin Zhao, "One-step robust deep learning phase unwrapping," Opt. Express **27**, 15100-15115 (2019)

Kaiqiang Wang, Qian Kemao, Jianglei Di, Jianlin Zhao, "Deep learning spatial phase unwrapping: a comparative review," Adv. Photon. Nexus 1(1) 014001 (3 August 2022)

Li, S., Xu, H., Gao, S., & Li, C. (2019). A non-fuzzy interferometric phase estimation algorithm based on modified Fully Convolutional Network. Pattern Recognit. Lett. 128, 60–69.

Liang, J., Zhang, J., Shao, J., Song, B., Yao, B., & Liang, R. (2020). Deep Convolutional Neural Network Phase Unwrapping for Fringe Projection 3D Imaging. Sensors 20, 3691.

Liang, Z.-P. (1996). A model-based method for phase unwrapping. IEEE Trans. Med. Imag. 15(6), 893–897.

Lin, Q., Vesecky, J.F., & Zebker, H.A. (1992). New approaches in interferometric SAR data processing. IEEE Trans. Geosci. Remote Sens. 30, 560–567.

Liu B, Wu L, Song X, Hao H, Zou L and Lu Y (2023) PUnet: A robust framework for phase unwrapping in interferometric SAR. Front. Environ. Sci. 11:1138399.

L. Zhou, H. Yu and Y. Lan, "Deep Convolutional Neural Network-Based Robust Phase Gradient Estimation for Two-Dimensional Phase Unwrapping Using SAR Interferograms," in *IEEE Transactions on Geoscience and Remote Sensing*, vol. 58, no. 7, pp. 4653-4665, July 2020.

SAR by the least-error path. Technical report, Johns Hopkins University Applied Physics Lab Technical Report, Laurel, MD, 1995.

M. Costantini, "A novel phase unwrapping method based on network programming", *IEEE Trans. Geosci. Remote Sens.*, vol. 36, no. 3, pp. 813-821, May 1998.

Pritt, M.D. (1994). Least-squares two-dimensional phase unwrapping using FFT's. IEEE Trans. Geosci. Remote Sens. 32, 706–708.

Perera, Malsha V., & De Silva, Ashwin. (2021). A Joint Convolutional and Spatial Quad-Directional LSTM Network for Phase Unwrapping. ICASSP 2021 - 2021 IEEE International Conference on Acoustics, Speech and Signal Processing (ICASSP, 4055-4059, 2021).

R. M. Goldstein, H. A. Zebker and C. L. Werner, "Satellite radar interferometry: Two-dimensional phase unwrapping," in *Radio Science*, vol. 23, no. 4, pp. 713-720, July-Aug. 1988.

SNAPHU: Statistical-Cost, Network-Flow Algorithm for Phase Unwrapping (https://web.stanford.edu/group/radar/softwareandlinks/sw/snaphu/)

Spoorthi, G., Gorthi, R.K.S.S., & Gorthi, S. (2018). PhaseNet: A deep convolutional neural network for two-dimensional phase unwrapping. IEEE Signal Process. Lett. 26, 54–58.

Spoorthi, G., Gorthi, R.K.S.S., & Gorthi, S. (2020). PhaseNet 2.0: Phase Unwrapping of Noisy Data Based on Deep Learning Approach. IEEE Trans. Image Process. 29, 4862–4872.

Teng Zhang, Shaowei Jiang, Zixin Zhao, Krishna Dixit, Xiaofei Zhou, Jia Hou, Yongbing Zhang, and Chenggang Yan, "Rapid and robust two-dimensional phase unwrapping via deep learning," Opt. Express **27**, 23173-23185 (2019)

Yan, L., Zhang, H., Zhang, R., Xie, X., & Chen, B. (2019). A robust phase unwrapping algorithm based on reliability mask and weighted minimum least-squares method. Opt. Lasers Eng. 112, 39–45.

Y. Qin et al., "Direct and accurate phase unwrapping with deep neural network," Appl. Opt., 59 (24), 7258 (2020).

M. Xu et al., "PU-M-Net for phase unwrapping with speckle reduction and structure rotation in ESPI," Opt. Lasers Eng., 151 106824 (2022).

Zhou, L., Yu, H., Lan, Y., and Xing, M. (2021). Deep learning-based branch-cut method for InSAR two-dimensional phase unwrapping. IEEE Trans. Geosci. Remote Sens. 10, 1–15.

Zhou, L.; Yu, H.; Lan, Y.; Xing, M. (2021). Artificial Intelligence in Interferometric Synthetic Aperture Radar Phase Unwrapping: A Review. IEEE Geosci. Remote Sens. Mag. 9, 10–28.

Zhou, L., Yu, H., Pascazio, V., and XingPU-Gan, M. (2022). A one-step 2-D InSAR phase unwrapping based on conditional generative adversarial network. IEEE Trans. Geosci. Remote Sens. 20.

Z.-P. Liang, "A model-based method for phase unwrapping," IEEE Trans. Med. Imag., 16 (6), pp. 893–897, Dec. 19

Citation

Saini, A., Mishra, D., Ramanujam V.M (2024). Phase Unwrapping Techniques for SAR Interferometry: A Comprehensive Review. In: Dandabathula, G., Bera, A.K., Rao, S.S., Srivastav, S.K. (Eds.), Proceedings of the 43rd INCA International Conference, Jodhpur, 06–08 November 2023, pp. 435–448, ISBN 978-93-341-2277-0.